Elsevier Editorial(tm) for Polymer

Manuscript Draft

Manuscript Number:

Title: Strain Amplitude Response and microstructure of PA /Clay Nanocomposites

Article Type: Regular Article

Keywords: Polyamide 6 , nanocomposites, microstructure

Corresponding Author: Dr mike John clifford The University of Nottingham

Other Authors: wan tong; Duncan Gregory; Fenge Gao; Andrew Bailey , , ,

Strain Amplitude Response and microstructure of PA /Clay Nanocomposites

W. Tong, M. J. Clifford*, F. Gao[a], A. S. Bailey,[b] D.H. Gregory [b]

School of Mechanical, Materials and Manufacturing Engineering,
[b]School of Chemistry,
The University of Nottingham, University Park, Nottingham, NG72RD, U.K.

[a]School of Biomedical and Natural Science, Nottingham Trent University, Clifton Lane, Nottingham, NG11 8NS, UK

*Email: mike.clifford@nottingham.ac.uk Telephone: +44 115 84661

Abstract:

PAn nanocomposites with various clay loadings were prepared by melt compounding in a twin extruder. Exfoliation of clay in a PA matrix was confirmed by X-ray diffraction. Strain Amplitude responses of PAn nanocomposites in both melt and solution states have been investigated. PAn nanocomposites were found to be very sensitive to the strain amplitude oscillatory shear. The logarithm of critical strain amplitude linearly decreases with clay loading and the strain amplitude response was reversible. Comparison of strain amplitude response in melt and solution state has been conducted. Two different responses have been observed: strain thinning in melt state and weak strain overshoot in solution state. Further studies showed that two types of interaction behaviors exist in nanocomposites: strain thinning which is dominant in nanocomposites caused by adsorption of PA chains on nanoclays and weak strain overshoot caused by weak bonds between PA chains and nanoclays.

Keyword: Polyamide 6 , nanocomposites, microstructure

1 Introduction

Polymer-clay nanocomposites have attracted considerable scientific and industrial interest because they exhibit significant improvements in physical and mechanical properties over virgin polymers with minimal increase in density [1]. Recently, much interest has focused on the rheological properties of polymer/clay nanocomposites based on the various polymer systems [2-5]. In general, two reasons drive the study of the rheology of nancomposites. From an engineering perspective, determining the rheological properties of nanocomposties is vital to optimize processing during manufacture of engineering components. It guides and improves melt processability to assist flow in molded parts and to impregnate continuous glass fibres to form composites with nanocomposites matrices. [6] From a scientific research point of view, nanocomposites provide an ideal nano-scale space to study the confined polymers and examine the effect of nano-fillers on the rheology of nanocomposites[7]. Furthermore, a thorough understanding of the rheological properties of nanocomposites is essential to tailor nanocomposites and governs the ultimate mechanical performance for various applications.

Previous studies on the rheology of nanocomposites showed that nanocomposites are sensitive to small deformation. They exhibit pseudo solid-like behavior and yield stress to a small oscillatory response. [8,9]. Higher viscosities and shear thinning properties can be observed for nanocomposites at relatively low shear rate at which the matrix exhibits a Newtonian response, but when the shear rate increases, the viscosities of nanocomposites decrease significantly [10]. The results can be attributed to the presence of anisotropic nanoclays forming a network structure, which can be broken down under large shear deformation. Since nanoclays significantly

affect rheology, the network formation would be related to the microstructure of nanocomposites and interaction between nanoclays and polymer matrix. However, the interaction and mechanism for formation of the microstructure are not readily understood.

Strain amplitude response of complex melts could reflect changes in microstructure of the melts and detect the complex interaction in melts. In general, the elastic (G') and the viscous (G'') modulus are chosen for characterizing the changes to the microstructure, so four types of strain amplitude responses to microstructure changes can be classified: type I, strain thinning (G', G'' both decrease); type II, strain hardening (G', G'' both increase); type III, weak strain overshoot (G' decrease, G'' increase followed by decrease); type IV, strong strain overshoot (G', G'' both increase followed by decrease)[11].

In order to explore the microstructure of nanocomposites, an experimental investigation was conducted to determine the strain amplitude response and recovery response of microstructure, for melts and solutions of PA/clay nanocomposites. PA/clay nanocomposites were studied because a high content of exfoliation takes place during the melt compounding process compared to other polymers [12,13]. In the high content of exfoliation system, an amount of clays in the form of single layer interacts with PA chains, providing a way to explore the interaction between nano-clay surfaces at the molecular level via rheology measurements. Strain amplitude measurements are a powerful method to probe the changes of the microstructure, especially when highly anisotropic layers are dispersed in a visoelastic matrix. In this paper, special emphasis is placed on strain amplitude response in melts and solutions and corresponding microstructure and the interaction.

2. EXPERIMENTAL METHOD

2.1 Materials

Ultramid B3 Polyamide 6 (PA) was supplied by BASF in the form of granules. Organo-clay (NTU-1) modified by organophilic surfactants was provided by Nottingham Trent University. All materials were dried at 80^{o}C under vacuum before testing.

2.2 Preparation of PA nanocomposites and nanocomposite solutions

PA and clay were melt blended at 240 ^{o}C in 16mm a twin screw extruder at feeding rate of 15%, L/D=24, 400rpm. The extruded strands were palletised and dried under vacuum at 80 ^{o}C for 10 hr before testing. Samples are denoted PA (for raw PA 6) and PAn where n=1,3,5,8,10 is the mass fraction of clay.

Nanocomposite solutions can be prepared by directly mixing PAn and 99% formic acid. First, 20g of PAn were dissolved in 80g of formic acid at 40 ^{o}C for three hours. The solution become light yellow transparent after PAn fully dissolved. In order to comparison, PAc (PA and clay) and PA solution were prepared as two references. The mixture of 18g PA and 2 g organo-clay (NTU-1) powder were added in 80 g of formic acid and mixed well to form PAc solution. 10g of PA dissolved in 90 g of formic acid to form PA solution.

2.3 Wide angle X-ray diffraction

Wide angle X-ray diffraction was used to measure the dispersion of clay in PA matrix. All data were collected using a Philips Xpert θ-2θ powder diffractometer in Bragg-Brentano, flat plate geometry with Cu Kα radiation. Samples were prepared for the diffraction experiment by cutting to the size of the plate aperture. The sample was then affixed to the plate by adhesive before performing the experiment. Data were collected for PA, the organo-clay (NTU-1) and all PAn samples as step scans from $1.5^{o} \leq 2\theta \leq = 30^{o}$ with a step of 0.02 ° and a time/step of 1.25 s. Peak positions and phase purity were evaluated using Philips APD and IDENTIFY routines respectively. Figure 1 shows WAXD patterns of NTU-1, PA and its nanocomposites. The d_{001} spacing for the clay was calculated automatically from Bragg's law, $n\lambda = 2d \sin\theta$.

2.4 Rheology characterization

Rheology tests were performed on a Bohlin CVOR200 Rheometer. A pair of 25 mm diameter parallel plates with a 1mm gap size was used in all tests. Strain amplitude sweeps were conducted from 0.1% to 100% at three different angular frequencies (ω = 0.5, 1 and 10 rad/s). The elastic modulus (G') and the viscous modulus (G'') as the function of the strain amplitude (γ) were recorded. In recovery measurements, frequency sweeps were carried out ranged from 0.1 to 100 rad/s at a fixed strain amplitude (γ=0.5%) to ensure that the measurements were taken within the linear visco-elastic range.

Sample disks for PAn with 1mm thickness were prepared by compression moulding of the extruded pellets at 240°C for 3 min. After loading between a pair of parallel

plates with 1mm gap, the sample disks were annealed for 5 minutes to ensure that they were fully melted and in an equilibrium state (240 ^{o}C). All measurements were conducted under a nitrogen atmosphere to avoid oxidative degradation.

Sample disks for PAn solutions were prepared by squeezing 3ml of solutions between a pair of parallel plates with 1mm gap and annealed for 5min. The measurements were carried out in 25^{o}C under a nitrogen atmosphere.

3. Results and discussion

3.1 **Characterization of exfoliation of PAn nanocomposites**

Figure 1 shows the WAXD patterns of the Organo-clay (NTU-1) and PAn nanocomposites. The organo-clay (curve a) has a sharp peak at 2θ = 3.6 ° corresponding to a [001] interlayer distance d_{001} = 2.45nm. Compared to the organo-clay, nanocomposites (cureves b-f) with various clay loading from 1-10 wt% do not exhibit an equivalent peak in the 2θ range of 2-10 ° . The absence of the [001] peak demonstrates that the clay is well dispersed within the PA matrix. Furthermore, in order to confirm the formation of nanocomposites, the crystalline patterns of PA and PAn nanocomposites have been studied in the range of 10-30°. Previous studies demonstrated that nanodispersed clays could affect the crystalline phase of PA, inducing a phase transition from the α- to the γ-polymorph. α crystalline phase has twin peaks at 20.3° (α1) and 23.7° (α2) while the peak of γ crystalline phase at 11 ° and 21.8°. [14,15] The observed X-ray diffraction patterns corroborate this previous

observation with the peak at 20.3° (α1) from the PA absent in nanocomposite samples. Figure 1 (curve g) shows that PA has both α and γ crystalline phase which corresponds to three peaks at 20.3°(α1), 21.8°(γ) and 24°(α2) respectively. However, PAn nanocomposites exhibit two peaks of γ predominance at 11° and 21.8° and conversely the absence of the peak at 20.3°, as shown in Figure 1 (b)-(f). The phase transition from α- to γ-polymorph is an additional strong indication of clay exfoliation and formation of nanoclays in PA matrix.

Figure 1

3.2 **Strain amplitude response and recovery of PAn nanocomposites in melt state**

To characterize the microstructure of PAn nanocomposites, the transitions from linear to nonlinear viscoelastic behaviours under strain amplitude have been studied. The strain amplitude dependence of the elastic modulus (G') for PA and PAn nanocompoistes were measured from 0.1% to 100% at the three frequencies ($\omega = 0.5, 1, 10\ rad/s$).The elastic modulus (G') of PA and PA10 are presented here as typical results. The elastic modulus (G') of PA and PA10 at different strain amplitudes are superposed with application of a normalized shift in Figure 2. Figure 2 shows that the elastic modulus (G') of PA and PA10 at different frequencies can be superposed and the transition of linear to nonlinear behaviour for PA10 is only a function of strain amplitude and is independent of frequency. All other nanocomposites measured also show the similar independent transition behaviours, so the critical transition of elastic modulus (G') can be denoted as critical strain amplitude (γ_c). For purposes of comparison of critical strain amplitude (γ_c), the elastic (G') and the viscous modulus (G'') of PAn nanocomposites were measured at the

same frequency and temperature ($\omega = 1 rad/s$ and 240 ^{o}C). The elastic moduli (G') of PAn nanocomposites are normalized by the values in the linear region at the low strain amplitudes and plotted against strain amplitude in Figure 3. The normalized elastic moduli (G') exhibit a linear region at low strain amplitude and nonlinear region at high strain amplitude. The region of linear viscoelastic behaviour for PA extends to a strain of 18%, but the presence of clay is very sensitive to small strains and causes the sharp decrease in the elastic modulus (G') for PAn nanocomposites beyond the critical strain amplitude (γ_c). An increasing clay loading resulted in lower critical strain amplitude (γ_c) and smaller linear visco-elastic range. The critical strain amplitude (γ_c) as a function of clay loading is shown in Figure 4. The critical strain amplitude (γ_c) gradually decreases with clay loading. The clay loading dependence of the critical strain amplitude (γ_c) can be explained by the formation of a network. Interestingly, network formation for nanocomposites occurs below the percolation threshold of composites. The critical loading of PA10 for the percolation is only 0.75%. Previous studies suggested that the anisotropic nanoclays could be aligned to the flow direction under strain amplitude and rupture clay particle-particle interaction [10]. Interestingly, Figure 4 shows that the logarithm of the critical strain amplitude decreases linearly with clay loading. We expected that the network structure in nanocomposites should gradually form with clay loading and probably be related to presence of either highly anisotropic clay or adsorption of PA chains on the filler network through organoclay- polymer chains interactions. The formation of a network is also related to the types of organoclay. Various organoclays can affect the rheological properties of eventual nanocomposites [17]. In order to explore the details of network formation and microstructure for PAn nanocomposites, the angular frequency sweeps ($\omega = 0.5 - 100 rad/s$) were performed at 0.5% strain amplitude to

make sure PAn nanocomposites have been measured in the linear region. The elastic moduli (G') shown in Figure 5 record the recoverable process of PAn nanocomposites, because they are sensitive to the angular frequency sweeps. The elastic moduli (G') of reversion are exactly the same as the first frequency sweeps. These results suggest that the network can rebuild quickly with the removal of the applied frequencies. The recovery of the network in nanocomposites may be due to the adsorption between nanoclays and PA chains. Obviously the adsorption is not as strong as crosslinked systems, since the complete recovery of the network only occurred in uncrosslinked polymer composites. As shown in Figure 2, the critical strain amplitude (γ_c) does not depend on frequency under strain amplitude. This demonstrates that the breakdown of the network is independent of the mechanical response of the PA matrix and is a function of clay loadings. We expect that a greater amount of nanoclays in the nanocomposites will encourage the adsorption of PA chains on the nanoclays. The interaction caused by the adsorption can be monitored by strain amplitude. In the small strain amplitude, the rate of adsorption is equal to that of desorption of PA chains on nanoclays. The elastic moduli (G') are constant in this equilibrium state. As the strain amplitude increases, the PA chains can be untangled from nanoclays and orient in the flow direction. Therefore, the threshold of strain thinning becomes more significant and the elastic moduli (G') decrease further in nanocomposites with increased clay loadings. This phenomenon suggests the adsorption exists between nanoclays and PA chains.

Earlier works [16] on end-tethered polymer layered-silicate nanocomposites showed that poly(caprolactone) nanocomposites at large strain amplitude (150%) for 3 hours, align in the flow direction. Because the clay particles dispersed in the polymer matrix as individual layers and stacks of layers are anisotropic particles with high aspect ratio

and quite large surface areas, the breakdown of the microstructure may be due to orientation of clay particles in the flow direction when shear is applied. Hydrotalcite-like/clay suspensions are time dependent viscoelastic composites. When shear is applied, thixotropic behavior occurs, that is, the viscosity depends on its previous shear history. [18,19] However, it is unlikely to observe the thixotropic behavior and the alignment of nanoclays in PAn nanocomposites during our tests, probably because the strain amplitude was only imposed for a relatively short time in which the obvious alignment of nanoclays can not be created.

Thus, the most reasonable explanation of strain amplitude response of PAn nanocomposite melts is that the large nanoclay surface easily absorbs PA chains and forms a physical network. It also worth noting that the end-tethered PCL nanocomposites exhibit shear thickening which is caused by the strong interaction between nanoclays and PCL chains. We believe that the special interaction exists between nanoclays and PA chains, even if it is not as strong as PCL nanocomposites. Only strain thinning of PAn nanocomposites could be observed in melt states, because the simple adsorption of PA chains on nanoclays which caused the adsorption points to disengage easily from nanoclays is dominant in PAn nanocomposites. Thus, the special interaction between nanoclays and PA chains cannot be easily observed in melt state.

3.3 **Strain Amplitude response of PAn solutions**

In order to explore the special interaction under strain amplitude, the simple adsorption must be weakening. The simple way to cut down the strain amplitude response of the simple adsorption is dissolution of PAn nanocompoites. In our tests,

formic acid was used to dissolve PAn nanocomposites. By this method, the clay loading in PAn solutions can be greatly diluted. For example, PA5 solution only has 1% clay loading. It not only reduces the interaction and the aggregation between nanoclays, but also substantially decreases the simple adsorption and entanglements of PA chains on nanoclays. However, the special interaction between nanoclays and PA chains is stronger than the simple adsorption. It is assumed that this special interaction becomes predominant in PAn solutions.

The elastic (G') and viscous (G'') moduli of PAn in melt and solution states respectively as a function of strain amplitude have been tested. To simplify the demonstration, the results for PA5 are presented here. The strain amplitude responses of PA5 in melt and solution state are shown in Figure 6. The elastic (G') and the viscous modulus (G'') both decrease for PA5 melts, which corresponds to strain thinning. However, the viscous modulus (G'') of PA5 solution increases and then decreases with strain amplitude while the elastic modulus (G') decreases. Obviously PA5 solution displays weak strain overshoot, so the weaker interaction exists between nanoclays and PA chains. In order to confirm the interaction caused by nanoclays and PA chains, additional measurements were carried out. PA solution, PAn solutions and PAc solution (the solution of mixture of PA and 10% organo-clay) were prepared as references by the same method. The viscous moduli (G'') of PAn solutions are shown in Figure 7. It is apparent that the viscous modulus (G'') of PAn solutions increases and then decreasing with strain amplitude. The weak strain overshoot becomes stronger with increasing clay loading, because more nanoclay surfaces interact with PA chains. PA1 solution only shows very small weak strain overshoot, but PA3, PA5, PA8 and PA10 show obvious weak strain overshoot and the interaction becomes significant. Figure 7 also exhibits that the critical transition of the viscous modulus (G'') from linear to nonlinear becomes smaller with increasing clay loading. This demonstrates that the interaction is dependant on clay loading. The interaction between nanoclays and PA chains become stronger with increasing nanoclays. In order to demonstrate the weak strain overshoot caused by the interaction between nanoclays and PA chains, PA and PAc solution have been studied. The results show in Figure 7. In contrast with PAn

solution, PA and PAc solutions just show Newtonian behavior instead of weak strain overshoot. The phase angles of these two solutions as a function of strain amplitude are shown in Figure 8. Compared to PA5 solution, the phase angles of PA and PAc solutions are nearly 90^{o} and independent of strain amplitude. These results demonstrate that PA chains and formic acid or nanoclays and formic acid do not have any strain amplitude response.

The fact that weak strain overshoot can be found in solution and not in the melt state can be explained by a bimodel response as shown in Figure 9. Most of PA chains are not bound to the clay layers, but there is physical adsorption on clay layers. In the melt state, this effect is dominant and results in strain thinning. On the other hand some of PA chains weakly bond to clay layers. In solution state, the physical adsorption is not as strong as in the melt state. The weak bond becomes dominant and results in weak strain overshoot.

4 Conclusions

Strain amplitude responses of PAn nanocomposites have been studied in both melt and solution states. The critical strain amplitude logarithm decreases with increasing clay loading. The elastic modulus of PAn nanocomposites is completely reversible under angular frequency sweeps. The weakly bonded interaction of PAn nanocomposite can be found in the form of weak strain overshoot. Two types of the interaction exist in PAn nanocomposites: strain thinning which is dominant in nanocomposites caused by adsorption of PA chains on nanoclay and weak strain overshoot caused by weak bonds between PA chains and nanoclays.

References:

[1] T.J. Pinnavaia, G.W. Beall, Polymer-clay nanocomposites, John Wiley & Sons Ltd, 2000; Chapter 6.
[2] Ramanan Krishnamoorti, Richard A.Vaia and Emmanuel P. Giannelis, Chem. Mater.,1996;8:1728-1734
[3] Jiaxiang Ren, Adriana S. Silva and Ramanan Krishnamoorti, Macromolecules, 2000; 33:3739-3746
[4] Girish Galgali, C.Ramesh, and Ashish Lele, Macromolecules, 2001; 34:852-858
[5] Jiaxiang Ren and Ramanan Krishnamoorti, Macromolecules, 2003; 36:4443-4451
[6] Daniel P.N. Vlasveld, Harald E.N. Bersee and Stephen J. Picken, SAMPE Europe Conference & Exhibition, 2004; 181-186
[7] E.P.Giannelis, R,Krishnamoorti,E.Manias, Advances in Polymer Science, Springer-Verlag Berlin 1999; 138:108-147
[8] Ramanan Krishnamoorti and Emmanuel P. Giannelis, Macromolecules 1997; 30: 4097-4102
[9] Yu Zhong and Shi-Qing Wang, Journal of rheology, 2003; 47(2): 483-495
[10] Ramanan Krishnamoorti, Jiaxiang Ren, and Adriana S.Silva, Journal of Chemical Physics, 2001; 114 (11): 4968-4978
[11] Kyu Hyum., Sook Heun Kim, Kyung Hyun Ahn and Seung Jong Lee, Journal of Non-newtonian Fluid Mechanics, 2002; 107: 51-65
[12] J.W. Cho and D.R. Paul, Polymer, 2001; 42: 1083-1094.
[13] Rhutesh K. Shah and D.R.Paul, Polymer, 2004;45: 2991-3000
[14] Xiaohui Liu and Qiuju Wu, Polymer, 2002; 43: 1933-1936
[15] Mutsumasa Kyotani, Journal of Polymer Science, 1979; 17: 103-114
[16] Ramanan Krishnamoorti and Emmanuel P. Giannelis, Langmuir, 2001; 17: 1448-1452
[17] kyung min lee and Chang Dae Han, Polymer 2003; 44: 4573-4588
[18] Shu-ping Li,Wan-guo Huo,De-jun Sun, Pei-zhi Guo and Chun-xiao Jia, Langmuir, 2003; 19: 3172-3177
[19] Ronald G.Larson, The structure and rheology of complex fluids, Oxford University Press, 1999 (Chapter 6)

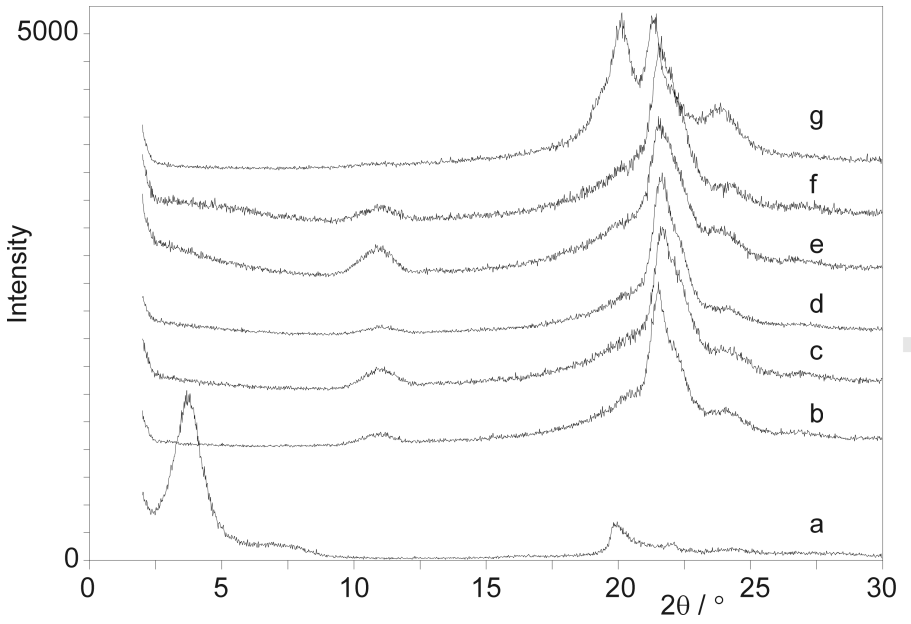

Figure 1. Powder X-ray diffraction profiles for Organo-clay (NTU-1) (a) and PAn nanocomposites, PAn, with mass fractions of clay, n=1, 3, 5, 8, 10 shown from (b)-(f) respectively. The diffraction pattern for PA is shown for comparison (g).

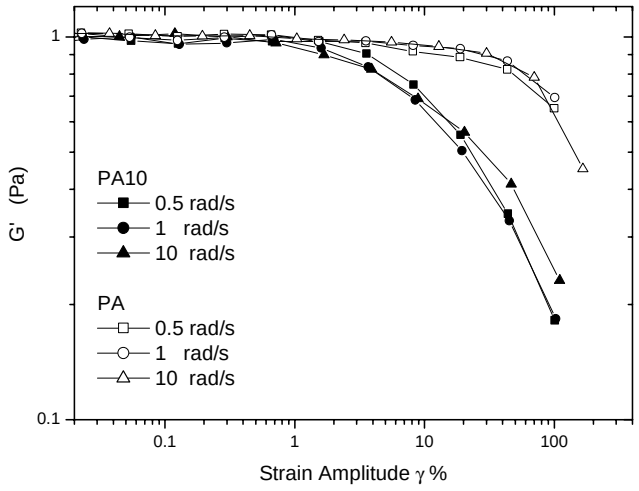

Figure 2 Strain amplitude dependence of the normalized elastic modulus of PA and PA10 at different frequencies 0.5, 1 and 10 rad/s (the open and closed symbols are for the PA and PA10, respectively)

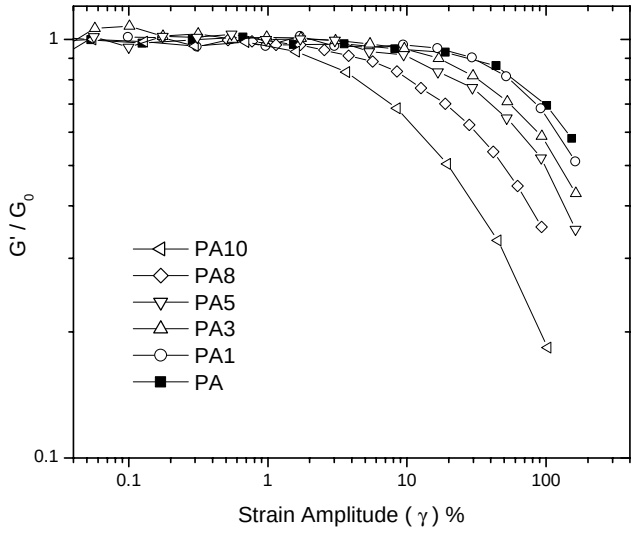

Figure 3 Strain Amplitude dependence of the normalized elastic modulus (G'/G_0) at a constant frequency ($\omega = 1 rad/s$) (the open and closed symbols are for the PA and PAn, respectively)

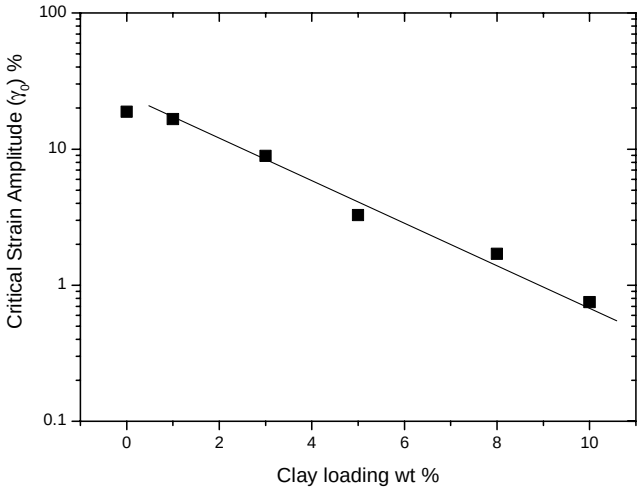

Figure 4 Critical strain amplitude (γ_c) as a function of clay loading

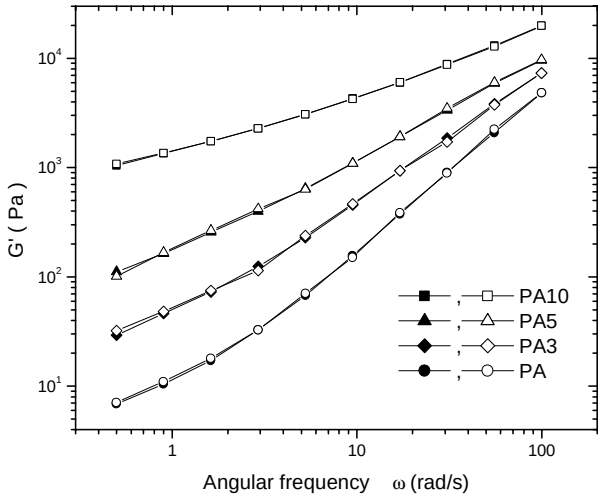

Figure 5 Elastic modulus (G') of PA and PAn as a function of angular frequency loop ($\omega = 0.5 - 100 rad/s$). The Open and closed symbols represent increasing and decreasing frequency sweeps respectively

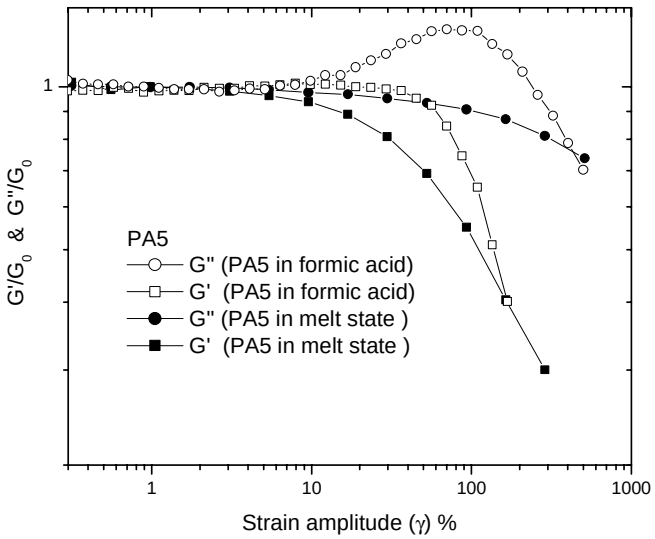

Figure 6. Reduced modulus G'/G_0 and G''/G_0 of PA5 melts and solution as a function of strain amplitude at $\omega = 1 rad/s$. PA5 in formic acid shows weak strain overshoot

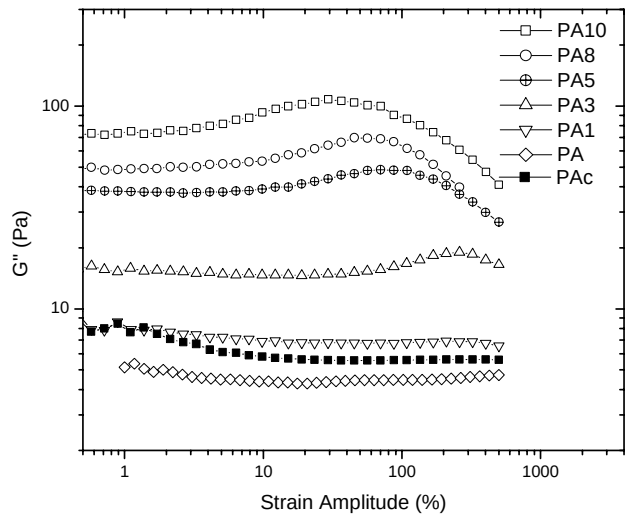

Figure 7 Viscous modulus G'' as a function of strain amplitude at $\omega = 1 rad/s$

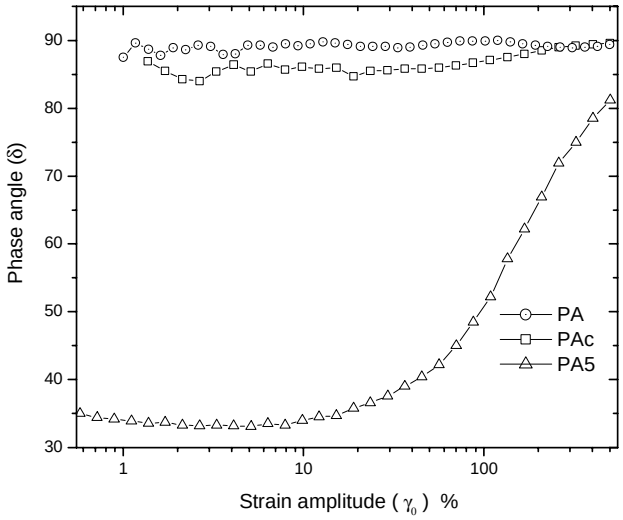

Figure 8 Phase angle as a function of strain amplitude, where PA and PAc (PA+10% organoclay) shows Newtonian behaviour

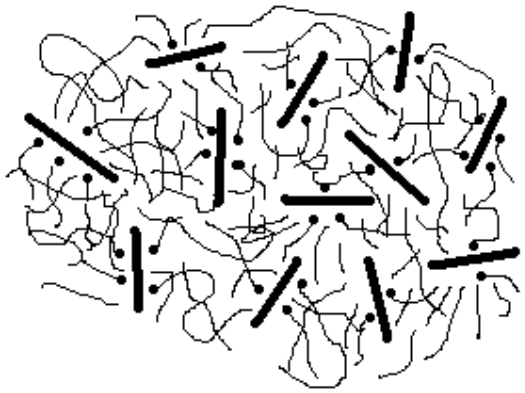

Figure 9. Schematic illustration of the PAn nancomposites with a close-up of the adsorption of PA chains on the nanoclays. Most of PA chains are not bound to the clay layers, but shows the physical adsorption on nanoclays. Some of the PA chains are weakly bound to nanoclays (black dots)